A Framework for Modeling Creep in Pure Metals

HOLGER BREHM and GLENN S. DAEHN

The process of creep in pure metals is modeled as the cooperative interaction of three phenomena: the thermally activated, force-dependent release of dislocation segments from obstacles; the substructrual refinement of the microstructure due to plastic deformation; and the diffusion-controlled coarsening of the substructure. Key parameters are given as approximate generic values which can be varied. It is shown that for a wide range of parameters, the model reproduces the key features of the creep of pure metals: a steady-state stress exponent near 5 is recovered, and the key microstructural-length scale is related by a power law close to the reciprocal of stress (this dependence is not a strong function of temperature at a given stress). In addition, the activation energy of steady-state creep is nearly that of self-diffusion. Thus, the model reproduces the well-known phenomenology of pure-metal steady-state creep. However, the present model is based on separate microstructural phenomena, which can be independently refined and studied.

I. INTRODUCTION

IT is remarkable that despite distinct differences in detailed mechanisms, all pure metals follow similar patterns of strength, rate sensitivity, and strain hardening as a function of temperature, strain, and strain rate. This has been clear since the seminal review of Sherby and Burke,[1] and many articles since this time have shown that by normalizing the strain rate by diffusivity, data taken over a wide range of temperatures and strain rates can collapse into a single line.[2–5]

The works of Sherby, Weertman, Dorn, and others[6–9] have been very compelling and collectively have taught us to see creep as being described as an equation of the form

$$\dot{\gamma}_{ss} = AD_{\mathrm{o}} \left(\frac{\tau}{\mu}\right)^{n} e^{-\frac{Q}{\mathrm{R}T}} \qquad [1]$$

where $\dot{\gamma}_{ss}$ is the steady-state strain rate, τ is the applied stress, μ is the elastic shear modulus, n is the stress exponent, Q is the activation energy for creep, T is the temperature, R is the gas constant, and A can be regarded as a fitting constant. By varying A, mildly varying n from its "typical" value of about 5, and mildly varying Q from its typical value of that for self-diffusivity, most data sets for pure metals in creep (and many for alloys and more complex materials) can be fit and rationalized. Often, if a good fit is not obtained, many groups have invoked modifications to this form, such as subtracting a threshold stress from the driving stress, which may itself be a function of temperature.

A key problem is that at its essence, Eq. [1] is a phenomenological fit to a large amount of data. It represents an approach that Oleg Sherby honestly refers to as "enlightened empericism."[11] It does not, however represent any distinct mechanisms, nor does it contain component parts that can be clearly removed, examined, and modified to possibly represent changes in varied materials, mechanisms, or conditions.

Presently, we propose a simple model of the creep behavior of pure metals. The model is numerical in nature because it is difficult to concurrently consider the required equations in closed form. This model reproduces the major features of the power-law creep of pure metals and the observed scaling behavior, using reasonable and measurable parameters and mechanistic relations as inputs. Further, we show that the model, being consistent with creep phenomenology, does not sensitively depend on the "correct" selection of parameters. Instead, reasonable behavior is obtained over a wide range of parameters.

II. BACKGROUND—THE PHENOMENOLOGY OF PURE-METAL CREEP

The key features of the creep of pure metals are summarized in the classic Sherby and Burke[1] review, and very recently, a comprehensive review was published by Kassner and Perez-Prado.[2] Typically, upon loading, the strain rate is quite large, and this causes an increase in dislocation density. Eventually, at a given strain, a steady-state creep region is usually obtained. Here, the strain rate does not vary with strain, and it is generally thought that the rates of dislocation accumulation and annihilation balance each other. Over the history of metal creep, experimental and theoretical approaches have emphasized "steady-state" creep, and a clear view of the phenomenology in this region has emerged. The essential features of steady-state creep at nominal temperatures between 0.5 and 1.0 of the absolute melting temperature are outlined in the following text.

A. *Stress Dependence*

From the most fundamental considerations of material strength, it follows that the flow stress should scale with the elastic shear modulus of the material. Accordingly, we can compare varied materials at applied stresses which are a given fraction of their shear moduli. It is well known that for applied stresses in the approximate range of τ/μ between

---

HOLGER BREHM, Visiting Scholar, and GLENN S. DAEHN, Professor, are with the Department of Materials Science and Engineering, The Ohio State University, Columbus, OH 43210.

This article is based on a presentation made in the workshop entitled "Mechanisms of Elevated Temperature Plasticity and Fracture," which was held June 27-29, 2001, in San Diego, CA, concurrent with the 2001 Joint Applied Mechanics and Materials Summer Conference. The workshop was sponsored by Basic Energy Sciences of the United States Department of Energy.

10^{-5} and 10^{-3}, most pure metals will exhibit a stress exponent of $n\left(n = \partial \ln \dot{\gamma}_{ss}/\partial \ln\left(\frac{\tau}{\mu}\right)\right)$ near 5 (usually, between 4 and 6). At lower stresses, experiments are difficult to perform because strain rates are very low. But at low stresses and high temperatures, the stress exponent often approaches unity. This region is called Harper–Dorn creep, after its discoverers,[12] and has been reviewed, for example, by Ardell[13] and Mohammed and Ginter.[14] At stresses at or above about 10^{-3} μ, the 5 power-law also often breaks down. Here, the strain rate increases exponentially with applied stress. A hyperbolic sine function raised to a power-law near 5 has long been known to describe the fit over a wide range of stresses, including the 5 power-law region and power-law breakdown.[3,4,15]

At relatively low temperatures, the stress exponent can often increase to a value near 7. This has been interpreted as a transition between creep controlled by lattice diffusion to dislocation pipe diffusion control[4] and will be discussed further in Section II–C.

B. *Substructure Dependence*

During deformation dislocations are generated, and at elevated temperatures these tend to cluster. At low temperatures, dislocations form thick, relatively disordered cell walls, whereas at higher temperatures (and higher strains), subgrains tend to be favored over cell walls. Thus, several distinct (but related) parameters can be used to characterize the microstructure, including the dislocation density and the cell or subgrain size. There have been numerous studies looking at these parameters in steady-state creep as a function of stress and temperature. The general conclusion of these studies is that the steady-state dislocation density generally varies approximately with the square of applied stress. Also, steady-state cell or subgrain sizes vary approximately inversely with applied stress. Typically, $(b/\lambda) = k(\tau/\mu)$, where k is a factor close to 1.[5,10,16,17] This factor, k, varies little, if at all, with temperature. A unified way to see this is that the characteristic microstructural dimension (either taken as λ or $1/\sqrt{\rho}$) varies approximately inversely with the applied stress, but is relatively insensitive to temperature.

One other result of this substructure dependence is a distinct difference between steady-state and constant-structure creep. Specifically, if a creep test is interrupted and the stress is increased, the immediate stress exponent will be much greater than 5 (*i.e.*, the material would be weaker than expected at the same stress in steady state). This is because the substructure generated by the lower stress applied before the stress increase represents a coarser, weaker substructure than the substructure established by applying the higher stress over a long period of time. Sherby *et al.* have suggested that the constant-structure stress exponent should be about 8. However, another school of thought developed by Biberger and Gibeling[18] suggests that constant-structure creep should be described as an exponential relationship between the stress and strain rate.

C. *Temperature Dependence*

The works of Sherby, Weertman, and others[1,4,6,19–22] have strongly made the case that steady-state creep is diffusion controlled. One particularly compelling piece of evidence in this regard is that if one takes creep data acquired over a range of stresses and temperatures and plots the data as $\log(\dot{\gamma}_{ss}/D)$ *vs* $\log(\tau/\mu)$ for most nearly pure metals, the data will collapse to a single trend line with a power-law exponent near 5. Here, D represents the diffusivity for the appropriate process and, as diffusivity is temperature dependent, $D = D_0 \exp(-Q/kT)$. The temperature dependence of the steady-state creep process seems to be explained by the temperature dependence of self-diffusivity. This scaling behavior has been demonstrated for many metallic systems.[1,4,6,10,23] One of the most remarkable demonstrations of this is provided by Luthy *et al.* in Figure 7 of their article.[4] In this case, the concept of an effective diffusivity is introduced and used. Here, diffusion through both the lattice and dislocation cores is considered. As a result of this, at low temperatures and high stresses, diffusion pipe paths are favored. The uncorrected stress exponent in these cases is about 7, because the volume fraction of pipe paths is proportional to the square of stress.

D. *Anomalous Systems and Unanswered Questions*

The basic phenomenology described previously is well supported in simple, nearly pure metals. However, there are many systems where the steady-state stress exponents are much greater than 5 and typically, in these systems, the activation energy for creep is much greater than that for self-diffusion. The systems that fall into this category typically have significant volume fractions of a second phase, as in the case of composites and creep-resistant engineering materials, which may have dispersion strengthening or a finely dispersed phase which can stabilize the substructure. The present model will include substructural refinement and coarsening processes which are typical for pure metals. The behavior of these creep-resistant materials is likely quite different than that for pure metals.

One last issue that is not well studied is related to the general phenomenology of creep in transient regions and, in particular, the value of the creep activation energy in primary creep. The Sherby–Burke review[1] makes the case that the activation energy remains constant over the entire creep curve (with relatively sparse supporting data), and this assumption is the basis of the Orr *et al.* life-prediction methodology.[7] In some circles, it seems that it has become conventional wisdom that the creep activation energy is constant with strain. However, there are very little data presently available to test this hypothesis. Indeed, there is evidence that in some cases the creep activation energy seems to increase systematically through the primary region.[24]

The model that will be presented below is largely consistent with this creep phenomenology.

III. MODELING APPROACH

The goal here is to couple accepted ideas on dislocation-obstacle bypass, structural refinement, and substructural coarsening into a coherent model of creep that describes the generic behavior of pure metals. The relations we will present are general and have free constants which can be tuned for specific situations. However, we will show that the basic results of the model are robust over a wide range of input parameters. Hence, the equations to follow are almost better regarded as coupled scaling relations than as strict descriptions of any particular material. The detailed mechanisms (which vary from material to material) are, of course, important in defining the behavior of that material and can be reflected in the specific equations and constants used in a model of this form.

We will consider one evolving microstructural parameter, the interobstacle spacing (λ), as describing the microstructure at any given point in time. We assume that this could equivalently be taken as $\rho^{-1/2}$.

We assume initially that plastic flow can be described by the classical equations for thermally activated bypass of dislocations over obstacles, where the energy barrier (ΔG^*) for overcoming an obstacle with a stress-free size (ΔF^*) and athermal bypass force ($\hat{k}$) is given by

$$\Delta G^* = \Delta F^* \left(1 - \left(\frac{f}{\hat{k}}\right)^p\right)^q \qquad [2]$$

where f is the force the dislocation exerts upon the obstacle and $\hat{k}$ is the force at which the dislocation would break free from the obstacle athermally. Equation [2] is a well-accepted description of the energy barrier a dislocation line must overcome to pass an obstacle.[25] We presently assume that all obstacles are identical and have characteristic values of ΔF^* and $\hat{k}$. Similarly, we assume that the force on all obstacles is the same and can be taken as

$$f = \tau \mathbf{b} \lambda \qquad [3]$$

where τ is the applied shear stress, λ is the interobstacle spacing, and $\mathbf{b}$ is the magnitude of the Burger's vector. In later work we will integrate this with an approach for dealing with obstacles of varied size and/or spacing, similar to a work published earlier.[26]

Dislocations overcome obstacles according to the usual Arrhenius rate law. That is, in a single atomic vibration period ($1/\nu$), the probability of overcoming the obstacle is given by

$$P_{\mathrm{slip}} = \exp\left(\frac{-\Delta G^*}{\mathrm{k}T}\right) \qquad [4]$$

where k is the Boltzmann's constant and T is the absolute temperature.

When the barrier is overcome, a strain increment is produced. We assume that obstacles make up something approximating a cubic array of obstacles with a characteristic spacing, λ. When a volume of λ on a side is sheared by a displacement of one Burger's vector, a shear strain on the order of $\mathbf{b}/\lambda$ is produced. Thus, at any given point in time, the material's strain rate can be written as

$$\dot{\gamma} = \frac{\mathbf{b}}{\lambda}\, \nu \exp\left(-\frac{\Delta F^* \left(1 - \left(\frac{\tau \mathbf{b} \lambda}{\hat{k}}\right)^p\right)^q}{\mathrm{k}T}\right) \qquad [5]$$

where $\dot{\gamma}$ represents the shear strain rate. Thus, with this simple approach, at any point in time we can predict a material's strain rate as a function of temperature, stress, and the character and spacing of the relevant obstacles.

We assume that the nature of the obstacles does not change with deformation. However, it is clear that the obstacle density must change with deformation. Plastic deformation operates dislocation sources, and these dislocations become pinned in the structure, causing strain hardening *via* structural refinement. Typically, this is modeled as an increase in the stored dislocation density using an equation of the form

$$\rho = \rho_0 + M \Delta \gamma \qquad [6]$$

where M is the dislocation breeding constant.

In the spirit of keeping the present model as simple as can be physically justified, we will use a single structural variable (which can be expressed as λ or ρ) to represent the material "hardness" or to represent the relevant microstructural scale in the material. Usually it is found that during primary creep, dislocations are rather homogeneously distributed, but they tend to cluster as the process goes on, forming cells and subgrains. In any case, the total dislocation density, the free dislocation density, and subgrain size all scale in a natural way with the applied stress. Nix and Ilschner[23] have clearly discussed these issues through the Taylor relation and the empirically determined relationship between applied stress and subgrain size. Based on dimensional arguments, the natural dislocation density and subgrain sizes can be related approximately as

$$\lambda = \frac{g}{\sqrt{\rho}} \qquad [7]$$

where, using Nix and Ilschner's arguments and the data of Staker and Holt,[27] for copper, the value of g should be taken as about 5. Generally, g can be seen as a measure of how readily free dislocations cluster into subgrains. A lower limit on g is $\sqrt{3}$, which represents the case where dislocations are evenly spaced, running orthogonally in three directions and meeting in a simple cubic lattice. If one increases the density of dislocations along one or more of the planes described in this lattice, the value of g will increase. This concept is supported by Figure 1. Thus, λ still represents the fundamental interobstacle spacing in the microstructure. While it seems that the nature of the dislocation pins must change with strain, the experimental evidence is that during steady-state creep, the average subgrain misorientation can change substantially with increasing plastic deformation; however, the creep strength changes little. It may be that while increasing the density of dislocations in the cell walls provides stronger traps for the dislocations, there is a nearly balancing effect, where the most weakly bound dislocation has about the same properties in this larger population. To re-emphasize, a particular model for the pin geometry is not formulated, but we believe the spacing should scale with and be similar to λ and/or $1/\sqrt{\rho}$.

At elevated temperatures, the dislocation networks that form subgrains will coarsen to reduce the total energy of the structure (seen as line or surface tension). While most models of creep have emphasized the dislocation-climb process as enabling deformation, here, the coarsening process is seen as the enabler of further flow. In a 1985 overview, Atkinson[28] compared the theories of grain growth in pure-metal, single-phase systems to experimental observations. It was found that over a time increment, the initial average grain size ($\overline{R}_0$) will grow to $\overline{R}_t$ as follows:

$$\overline{R}_t^m - \overline{R}_0^m = Kt \qquad [8]$$

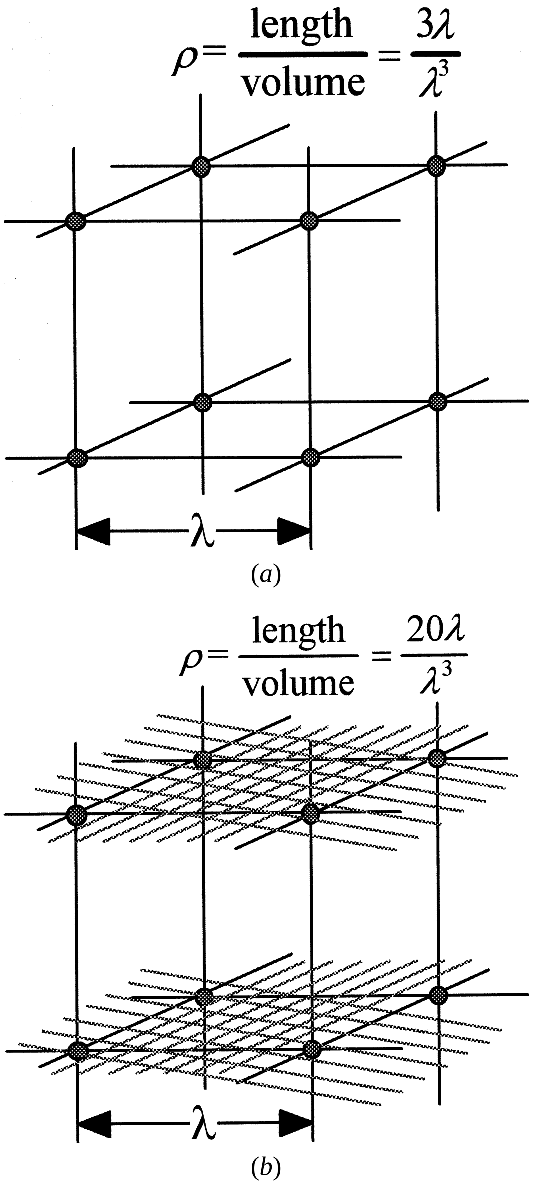
$\rho = \frac{\text{length}}{\text{volume}} = \frac{3\lambda}{\lambda^3}$
λ
(a)
$\rho = \frac{\text{length}}{\text{volume}} = \frac{20\lambda}{\lambda^3}$
λ
(b)

Fig. 1—(*a*) The greatest possible dispersion of dislocations in space. Here, they form a cubic array where dislocations are evenly spaced in the *x, y,* and *z* directions, in which case *g* in Eq. [7] is equal to $\sqrt{3}$. In case (*b*), dislocations are arranged in planar arrays along one set of planes. Here, *g* is equal to about $\sqrt{20}$.

where $\bar{R}$ is the average grain size, K is a fitting constant, and t represents time. The grain-growth or coarsening exponent (m) is particularly interesting. The classical value of m is 2, which comes from the seminal paper of Burke and Turnbull.[29] However, both experiments and models that consider the interplay of the topological requirements for space filling with growth kinetics show that a wider range of exponents is available. For example, models commonly show values of this exponent between 2 and 4. Experimental data show the same range with several metals, showing exponents near 2.5 to 3, and aluminum has shown a value as high as 4. We are presently assuming that grains and subgrains behave similarly. But values for energy and mobility are different. Subgrains may also have longer-range stress fields associated with them. It is also important to note that this form of coarsening equation has been shown to be quite general. It has been used to describe diverse systems such as precipitates,[30] thin films,[31,32] and phase separation in copolymer blends.[33] One theme that persists in this work is that a range of coarsening exponents is available, depending on detailed conditions.[34]

In our implementation of the model, we adapt Eq. [8] for describing coarsening of the substructure parameter, λ:

$$\bar{\lambda}_{dt}^{m_c} - \bar{\lambda}_{0}^{m_c} = KDdt \qquad [9]$$

where D represents self-diffusivity. This is, of course, temperature dependent and may or may not include dislocation pipe diffusion and boundary diffusion in addition to lattice diffusion.

Parameters and Implementation of the Model

The goal of this model is not to carefully consider the creep behavior of a particular material, but instead to consider the generic aspects of pure-metal creep. Accordingly, we assume that a material is characterized by its shear modulus, and the magnitude of the Burger's vector. From here, we assume melting-point scales with a modulus as $T_m = \mu \mathbf{b}^3/(48\ \mathrm{k})$, where k is the Boltzmann's constant.

For diffusion, we assume that the "generic" behavior of metals as discussed in Shewmon[35] holds. Thus, for most metals, their diffusivity can be roughly expressed at their homologeous temperature ($T_h = T/T_m$) as

$$D = 2\mathbf{b}^2\ \nu \exp\left(\frac{-12}{T_h}\right) \qquad [10]$$

With this form at the melting point, the diffusivity of metals will be about $10^{-12}\ \mathrm{m^2 s^{-1}}$, which is suggested as an empirical rule of thumb.[35] Presently, we shall neglect the possible effects of dislocation pipe diffusion or other internal short-circuit paths. However, the model can be easily modified to accept this refinement, and it does not change the basic results we will present.

Again, we assume that $\mu \mathbf{b}^3 = 48\ \mathrm{k}T_m$. With the normalizing used presently, the diffusion activation energy becomes $0.45\ \mu \mathbf{b}^3$. Further, we normalize by assuming $\Delta F^* = s_1\ \mu \mathbf{b}^3$ and $\hat{k} = s_2\ \mu \mathbf{b}^2$, where s_1 and s_2 can be considered to be either material properties or properties of the particular obstacle determining the energy required for a dislocation required to overcome an obstacle. If two dislocations simply intersect to form two-unit jogs, this requires an energy of about 1/4 to 1/2 $\mu \mathbf{b}^3$ ($0.25 \leq s_1 \leq 0.5$). However, it is much more common for dislocations to interact strongly in subboundaries. For example, it is common in bcc metals for two a/2 ⟨111⟩–type dislocations to form an attractive junction, making a full ⟨100⟩-type dislocation. Junctions such as these may be quite energetically stable and could be responsible for s_1 values much greater than unity. The athermal strength of the obstacle is represented by s_2. If the dislocation line tension is taken as $\mu \mathbf{b}^2$, then s_2 can be taken as the cosine of the athermal obstacle breaking angle. Thus, s_2 is formally bounded between zero and unity (*i.e.,* bypass takes place at $s_2 = 1.0$). However, one could justify $s_2 > 1$ to possibly account for obstacle clustering.

IV. RESULTS

The equations developed were used in two different modes, with two different models to develop the evolution

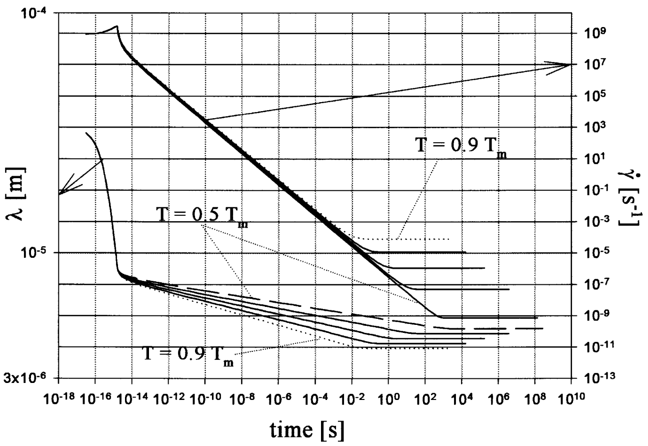

Fig. 2—Behavior of the structural parameter λ and the strain rate with increasing time. The bottom left shows λ as a function of time. The upper right graphs show the development of the strain rate $\dot{\gamma}$. In all cases, $\tau/\mu = 1.6 \times 10^{-5}$; $T/T_m = 0.5, 0.6, 0.7, 0.8,$ and 0.9; and the standard parameters in Table I are used. Note that the model shows a clear steady-state regime after a transient.

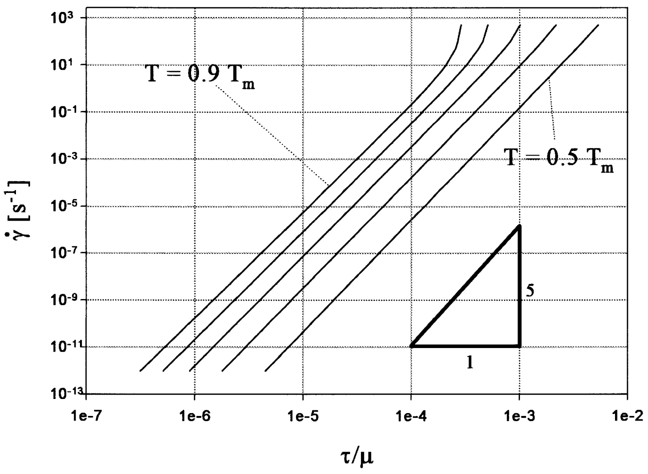

Fig. 3—Predicted steady-state strain rate as a function of applied stresses at $(T/T_m) = 0.5, 0.6, 0.7, 0.8,$ and 0.9. Constants used in Table I are used throughout.

Table I. Parameters and Values Used in the Model Except Where Stated Otherwise

Parameter	Corresponds to	Value	Units	Used as
b	Burgers vector	$2.775\ 10^{-10}$	m	Eq. [3]
v	atomic vibration frequency	10^{14}	s^{-1}	Eq. [5]
s_1	obstacle energy parameter	1.5	—	Eq. [5]
s_2	athermal force parameter	0.5	—	Eq. [5]
m_c	grain growth exponent	3	—	Eq. [9]
M	dislocation breeding constant	10^{17}	m^{-2}	Eq. [6]
g	dislocation subgrain relation parameter	5	—	Eq. [7]
p	obstacle aspect ratio constant	1	—	Eq. [2]
q	obstacle shape parameter	$\frac{3}{2}$	—	Eq. [2]

of λ and $\dot{\gamma}$, respectively, and to find steady-state values. This is described sequentially in Sections III–B and C.

A. *Approach to Steady State by Evolution of λ and $\dot{\gamma}$*

Here, we start with an initial dislocation density of 2.5 10^{10} m^{-2} (or, equivalently, a microstructural dimension (λ) of about 32 μm). A time-stepping procedure is used, and small strain increments are added at discrete times using Eq. [5]. Also, at each time increment, Eqs. [6] and [9] are used to modify ρ and λ. As an example, Figure 2 shows the results of a simulation carried out at an applied stress of 1.6×10^{-5} μ; homologeous temperatures of 0.5, 0.6, 0.7, 0.8, and 0.9 T_m; and the materials parameters shown in Table I. Plotted on linear axes, the strain-time curve looks like a fairly ordinary creep curve with fast plastic flow and decelerating creep into steady state, except that at all temperatures steady state is reached at a very low strain of about 0.1 pct. Figure 2 shows the resulting strain rate on log-log axes. The initial part of the strain (up to about 2×10^{-6}) places forces on obstacles that exceed the athermal strength of the obstacles, and deformation is very fast. After this initial period, the dislocation density rises to the point where thermal activation is required to overcome barriers, and the strain rate slows systematically with increasing strain. If this model is run at a constant strain rate instead of fixed stress, we find that the model provides a strain-hardening exponent of about 0.5, irrespective of strain rate or temperature. Eventually, a steady state is obtained where the recovery and hardening processes balance. This is shown by the clear constant strain rate in Figure 2. Figure 2 also shows the evolution of the characteristic spacing, λ. Note that both λ and $\dot{\gamma}$ reach values that do not change in steady state. Also, steady-state values of λ and $\dot{\gamma}$ are weak functions of the normalized temperature.

B. *Steady-State Behavior*

A separate routine models steady-state behavior. Starting with a target strain rate, Eqs. [6], [7], and [9] are used to numerically solve for the value of λ that is obtained in steady state at a given temperature for a given set of materials parameters. Once λ is known, Eq. [5] can be used to numerically solve for τ at the given strain rate, with all the other parameters known. This provides a very efficient method to determine steady-state creep rates over a wide parameter space, and the results are fully consistent with those developed from the evolution approach described previously.

Figure 3 shows the strain rate plotted as a function of τ/μ for temperatures between 0.5 and 0.9 T_m. At the lower temperatures the trend line is quite linear, with a slope of about 5 on the log-log axes. At higher temperatures, there is deviation from the 5 power law at both the higher and lower strain rates. In Figure 4, the strain rate is now normalized by the diffusivity. This causes the data to largely collapse to nearly a single scatter band. The data collapse most fully at a stress between 10^{-5} and 10^{-4}. At higher and lower stresses, the curves diverge with higher temperatures, showing deviations like those seen in Harper–Dorn creep and power-law breakdown at low and high stresses, respectively. This divergence becomes stronger as s_1 is decreased.

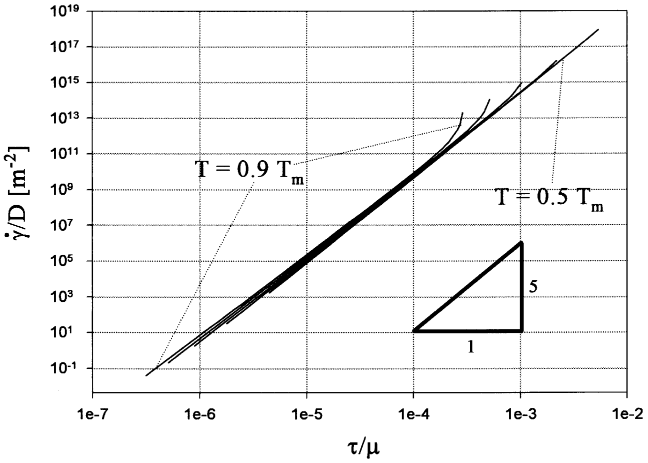

Fig. 4—Same data as in Fig. 9 except now steady-state strain rate is divided by diffusivity at the test temperature. This causes the data to collapse to nearly a single trend line.

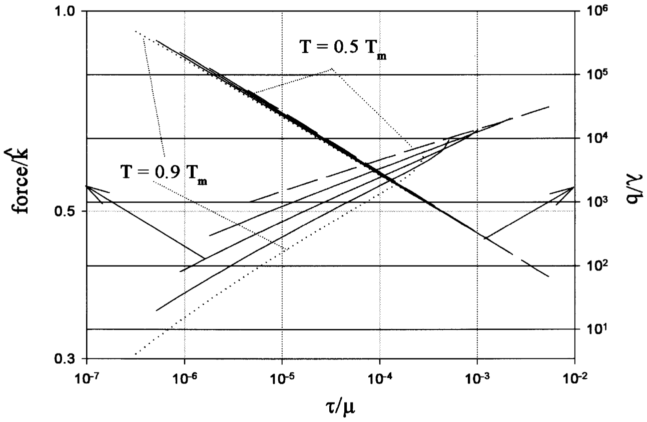

Fig. 5—These are again results from the same simulations presented in Figs. 9 and 10. Here, normalized force $f/\hat{k}$ is presented as one axis. There is a rising trend in this data set. The term λ is presented on the other axis. Note these data taken at varied temperatures collapse well. This shows $(\lambda/\mathbf{b}) \approx \mathrm{k} \cdot \left(\frac{\mu}{\tau}\right)$.

Figure 5 shows how the normalized force $(f/\hat{k})$ and subgrain size in steady state vary with applied stress over the range of temperatures simulated. Note that at stresses between 10^{-5} and 10^{-4}, where the normalized strain rates converge best (even for lower s_1 values), the normalized force and subgrain sizes are nearly independent of temperature. Also, the breakdowns in the power-law behavior take place as the normalized force approaches zero and 1, respectively, at low and high applied stresses. Notice that in general, the variation of normalized force with temperature is greater at higher temperatures, accounting for the reduced power-law regime.

The effect of varying parameters on the normalized strain rate as a function of applied stress is studied in Figure 6. In all cases, the parameter set used in Table I is used, with the exception of changing the selected values highlighted in each graph. The effect of obstacle strength on creep behavior is examined in Figure 6(a). Increasing the obstacle size increases the creep strength, and increasing the energy barrier improves the degree to which data taken at varied temperatures collapse to a single trend when normalized by

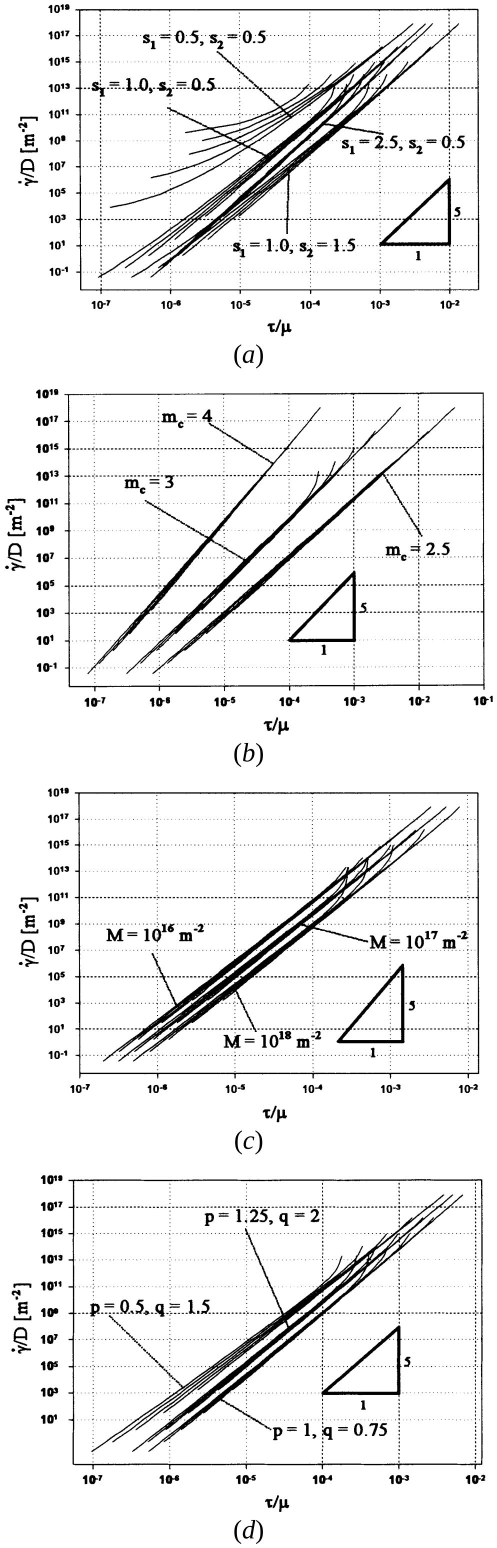

(a)

(b)

(c)

(d)

Fig. 6—The effect of variation of the model parameters on the normalized strain rate as a function of stress is considered. All parameters except those varied chosen according to Table I, $(T/T_m) = \{0.5, 0.6, 0.7, 0.8, 0.9\}$. (*a*) Increasing obstacle strength through s_1 and s_2 increases materials' strength, and increasing s_1 improves the convergence of the normalized data. (*b*) The effect of variation of the coarsening exponent, m_c, on the normalized strain rate as a function of stress is considered. (*c*) Shows that increasing the dislocation breeding constant, *M*, increases materials' strength. (*d*) The effect of variation of the exponents *p* and *q* on the normalized strain rate as a function of stress is considered. Changes in these exponents are relatively unimportant. In all cases, the most highly curved lines correspond to the highest temperature.

diffusivity. Note that even when ΔF^* is near the activation energy for self-diffusion (0.45 *vs* 0.5 $\mu \mathbf{b}^3$), the data collapse by a reasonable degree. Also, as s_1 increases beyond 5, the 5 power law is maintained, but the trends no longer shift to lower strain rates with increasing energy barrier size. The variation of the coarsening exponent (m_c) is considered in Figure 6(b). Here, we vary the coarsening constant, K, in Eq. [9] with m_c in such a manner that in 1000 seconds, at the melting temperature, very fine microstructural spacing would coarsen to 100 μm. Generally, increasing the value of the coarsening exponent increases the stress exponent (n), causes the normalized creep data to collapse better to a trend, and reduces the material creep strength (because structures finer than 100 μm will coarsen faster at increased m_c values). However, the change in stress exponent with coarsening exponent is fairly mild. For the conditions shown here, n increases from about 4.1 to 5.7 when m_c varies between 2.5 and 4. A recent closed-form analysis shows a limiting value of $n = m_c + 2$ develops as s_1 becomes large.[39] Changing the values of the constants in these equations usually has the effect of largely shifting the trend lines. For example, Figure 6(c) shows the effect of varying the dislocation breeding constant between 10^{16} and 10^{18} m^{-2}. The increased rate of dislocation generation causes the structure to refine better, increasing the material strength. The value of the stress exponent and other characteristics are quite similar. Last, Figure 6(d) shows that the values of p and q in Eq. [2] have little effect on the simulations. In summary, Figure 6 shows that the steady-state strain rate *vs* stress characteristics are similar over a wide range of input values. The steady-state stress exponent remains near 5 for stresses nominally between 10^{-5} and 10^{-3} μ. Also, the strain rate normalized by diffusivity tends to collapse to one trend line for values of s_1 which are significantly greater than 0.45 (which represents the activation energy for plastic flow being greater than that for diffusivity).

Figure 7 shows the predicted variation in λ with applied stresses for temperatures between 0.5 and 0.9 T_m, with a variety of parameter sets. Basically, the graphs show that each simulated material (represented by a given parameter set) behaves in accord with known creep phenomenology. Data developed at varied temperatures collapse into a relatively narrow trend. Also, there is a nearly inverse relationship between λ and the applied stress. In this particular case, the relationship is closer to $\lambda = k\,(\tau/\mu)^{-p}$, where the value of the exponent p is approximately 0.9 for the standard parameters at stresses between 10^{-5} and 10^{-3} μ. This exponent value is within experimental error for many measured data sets of subgrain size as a function of stress, reviewed by Takeuchi and Argon.[36]

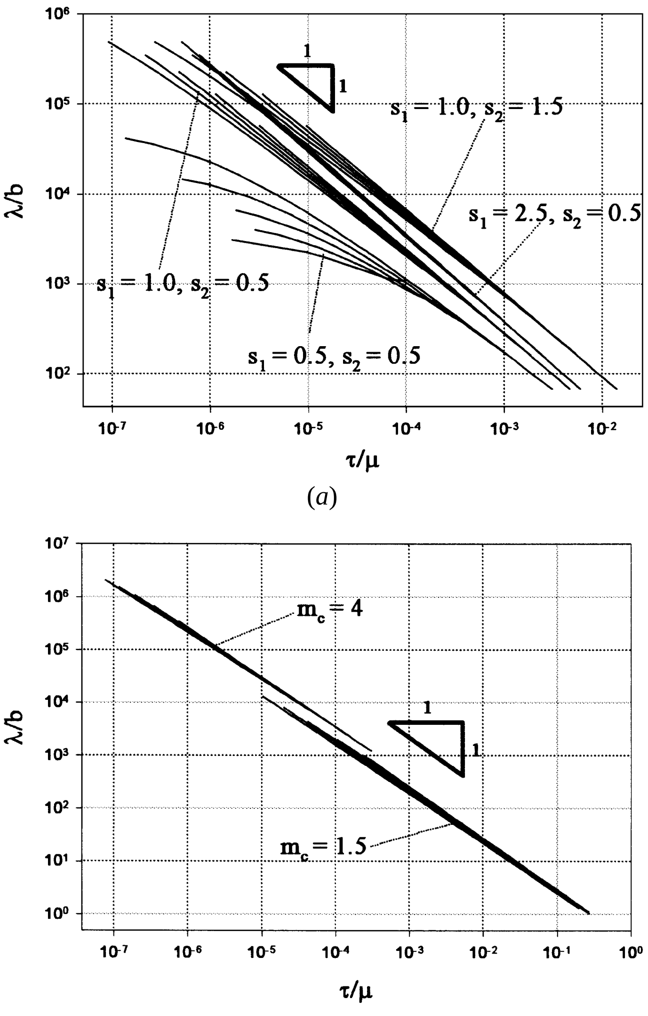

(*a*)

(*b*)

Fig. 7—$\lambda/\mathbf{b}$ as a function of applied stress. (*a*) Increasing obstacle strength increases λ and also increases the degree of data convergence. (*b*) The value of the coarsening exponent, m_c, is relatively unimportant in setting the slope of this curve. In all cases, conditions in Table I are used and $(T/T_m) = \{0.5, 0.6, 0.7, 0.8, 0.9\}$.

IV. DISCUSSION AND OPEN QUESTIONS

Overall, the trends shown in Figures 2 through 7 are in very good agreement with well-known creep phenomenology. The creep activation energy is very close to that for self-diffusion. The stress exponent robustly takes on values near 5 over a wide range of input parameters, stresses, and temperatures. The characteristic microstructural scale varies nearly inversely with applied stress. These are results from the model; these are not characteristics that were explicitly built into the model. Even with the crude approximations made presently, the model's absolute values are in rough accord with absolute values of creep rates. The 1962 review by Sherby[37] shows that, for a number of metals, when creep data are plotted as $\dot{\gamma}/D$ *vs* σ/E, the main trend line has a slope near 5 and falls approximately through a stress of $\sigma/E = 10^{-4}$ at $\dot{\gamma}/D = 10^{10}$ m^{-2} (plus or minus a couple of orders of magnitude). This is in good accord with the present predictions, as shown in Figure 6. Also, Figure 7 shows reasonable agreement with experimentally measured trends. Takeuchi and Argon have reviewed the steady-state subgrain sizes in the creep of several materials and have concluded that an equation of the form $\lambda = k(\tau/\mu)^{-p}$ is appropriate where p should be in the range of 0.7 to 1, when τ is about 10^{-4} μ, and steady-state subgrain sizes range between 10^5 and 10^6 $\mathbf{b}$. For most metals, there is only a small temperature dependence on subgrain size. In our case, the microstructural dimension, λ, is smaller than the typical subgrain size predicted by these trend lines by one order of magnitude or more. The parameter λ, here, does not explicitly represent subgrain size, and this may simply be because the relevant microstructural spacing is the pin spacing within the subgrain wall, which is, of course, smaller than the subgrain size. All of this is encouraging for a model which is only expected to have, at best, order-of-magnitude predictive capability.

This model is posed in a rather general way to capture the trends that seem common to all nearly pure single-phase metals, and it is supposed that the differences between systems can be explained by matching the exact equations and parameters to microstructural mechanisms. One issue that is troubling is that we do not have a coherent view of what the nature, spacing, and strength characteristics of the discrete pins are. Often it is thought that, for pure metals, ΔF^* should be less than 0.5 $\mu \mathbf{b}^3$ for typical forest-type interactions. However, if the fundamental activation energy for dislocation release is equivalent to or less than that for self-diffusion, it would be very difficult to explain why creep activation energies are not significantly smaller than those for self-diffusion, and it would also be difficult to explain why materials are as strong as they are at elevated temperatures. It seems quite possible for dislocation intersections to relax into networks and junctions of quite low energy, which are difficult to overcome. In most engineering creep-resistant materials, particles or second phases are introduced which largely hinder the dislocation or subgrain coarsening processes. In most metal matrix composites (MMCs), these particles are far too large to interact with individual dislocations. The fact that most MMCs and creep-resistant materials show creep activation energies that are much greater than those for self-diffusion is an indication that, typically, activation energies for dislocation release are greater than those for self-diffusion. The fact that the stress exponents are also typically much greater than 5 in these cases (as well as in constant-structure creep) is also consistent with this explanation.

Another problem related to our limited understanding of the nature, spacing, and geometry of the pins is that it is, thus, difficult to formulate a model for the coarsening of these features. However, the form of Eq. [9] is quite general and can be applied to many coarsening processes. It is expected that the constant K and coarsening exponents may be related to the specific material as well as to parameters such as the stacking-fault energy, which should have a strong effect on the nature of the pinning sites as well. In principle, mechanical interrogation experiments, where samples in the steady-state regime are unloaded for controlled periods of time and reloaded with initial strain rates measured, could be used to study this pin-coarsening process. One must also be wary of the fact that recovery processes may be significantly accelerated by stress, as argued by Takeuchi and Argon.[36]

It is also appealing and interesting that this model seems to suggest that power-law breakdown and Harper–Dorn creep may be natural consequences of a change in the nature of these equations as $f/\hat{k}$ becomes close to its bounding values of zero or one. It is also interesting to ponder if the power-law breakdown regime has the same activation energy as for self-diffusion. This model suggests that it may not, and there is little firm support one way or the other in the literature. We will not speculate on power-law breakdown or Harper–Dorn creep further at the present time.

Last, one aspect of this model that is clearly not presently satisfactory is the transient response. Important issues such as backflow or Bauschinger effects cannot be accounted for. Also, the apparent strain-hardening exponent in this model is nearly fixed at 0.5 and changes abruptly at steady state. It seems such issues may be handled by introducing a distribution of pin strengths with a load redistribution similar to an approach published earlier.[26] These approaches will be integrated with the present model and presented in the near future.

V. CONCLUDING REMARKS

We have developed a model for creep that is composed from separate equations for dislocation bypass of obstacles, structural refinement by plasticity, and structural-diffusion-controlled coarsening. The model recovers well-known creep phenomenology. Significant effort can still be justified to gain a better understanding of these constituent processes.

ACKNOWLEDGMENTS

This work was supported by the National Science Foundation under Award No. DMR-0080766. Also, a von Humboldt Foundation grant funded the work of Holger Brehm. We acknowledge many useful interactions with Professor Michael Mills on this work, and Professor Yunzhi Wang helped give direction on coarsening. The old-school training of the reviewer was apparent in many useful suggestions. Unser herzlicher Dank gilt der Alexander von Humboldt Stiftung Bonn/Bad Godesberg fuer die Gewaehrung eines Feodor Lynen Forschungsstipendiums, durch das diese Arbeit ermoeglicht wurde.

REFERENCES

1. O.D. Sherby and P. Burke: *Progr. Mater. Sci.*, 1967, vol. 13, p. 325.
2. M.E. Kassner and M.T. Perez-Prado: *Progr. Mater. Sci.*, 2000, vol. 45, pp. 1-102.
3. J. Cadek: *Materials Science Monographs*, Elsevier New York, NY, 1988, vol. 48.
4. H. Luthy, A.K. Miller, and O.D. Sherby: *Acta Metall.*, 1980, vol. 28, p. 169.
5. J.P. Poirier: *Creep of Crystals, High Temperature Deformation Processes in Metals, Ceramics and Minerals*, Cambridge University Press, New York, NY, 1985.
6. O.D. Sherby and J. Weertman: *Acta Metall.*, 1979, vol. 27, p. 387.
7. R.L. Orr, O.D. Sherby, and J.E. Dorn: *Trans. ASME*, 1954, vol. 46, p. 113.
8. J. Weertman: *J. Appl. Phys.*, 1955, vol. 26, p. 1213.
9. J. Weertman: *J. Appl. Phys.*, 1957, vol. 28, p. 362.
10. A.K. Mukherjee: in *Treatise on Materials Science and Technology*, R.J. Arsenault, ed., Academic Press, New York, NY, 1975, vol. 6, p. 163.
11. O.D. Sherby: personal communications, 1984-88.
12. J.G. Harper and J.E. Dorn: *Acta Metall.*, 1957, vol. 5, p. 654.
13. A.J. Ardell: *Acta Mater.*, 1997, vol. 45, pp. 2971-81.
14. F.A. Mohamed and T.G. Ginter: *Acta Metall.*, 1982, vol. 30, p. 1869.
15. J. Weertman: *Proc. 2nd Int. Conf. Creep and Fracture in Engineering Materials and Structures*, B. Wilshire and D.R.J. Owen, eds., Pineridge Press, Swansea, 1984, p. 1.
16. K.D. Challenger and J. Moteff: *Metall. Trans.*, 1973, vol. 4, pp. 749-59.
17. C. Perdrix, Y.M. Perrin, and F. Montheillet: *Mem Sci. Rev. Metall.*, 1981, vol. 78, p. 309.
18. M. Biberger and J.C. Gibeling: *Acta Metall. Mater.*, 1995, vol. 43, pp. 3247-60.
19. S.L. Robinson and O.D. Sherby: *Acta Metall.*, 1969, vol. 17, p. 109.
20. C.R. Barrett and O.D. Sherby: *Trans. AIME*, 1964, vol. 203, p. 1322.
21. P.M. Burke, W.R. Cannon, and O.D. Sherby: *J. Mater. Sci.*, 1968.
22. J.E. Breen and J. Weertman: *Trans. AIME*, 1955, vol. 203, p. 1230.
23. W.D. Nix and B. Ilschner: in *Strength of Metals and Alloys*, P. Haasen, V. Gerold, and G. Kostorz, eds., Pergamon Press, Oxford, United Kingdom, 1980, p. 1503.

24. R.P. Carreker: *J. Appl. Phys.*, 1950, vol. 21, pp. 1289-96.
25. U.F. Kocks, A.S. Argon, and M.F. Ashby: *Proc. Mater. Sci.*, 1975, vol. 19.
26. G.S. Daehn: *Acta Mater.*, 2001, vol. 49 (11), pp. 2017-26.
27. M.R. Staker and D.L. Holt: *Acta Metall.*, 1972, vol. 20, p. 569.
28. H.V. Atkinson: *Acta Metall.*, 1988, vol. 36 (3), pp. 469-91.
29. J.E. Burke and D. Turnbull: *Progress in Metal Physics*, Pergamon Press, London, 1952, vol. 3, p. 220.
30. C.S. Jayanth and P. Nash: *J. Mater. Sci.*, 1989, vol. 24, 3041-52.
31. A. Siegert: *Phys. Rev. Lett.*, 1998, vol. 81, pp. 5481-84.
32. P. Smilauer and D.D. Vvedensky: *Phys. Rev. B*, 1995, vol. 52 (19), pp. 14263-14272.
33. L. Sung, A. Karim, J.F. Douglas, and C.C. Han: *Phys. Rev. Lett.*, 1996, vol. 76, pp. 4368-71.
34. B. Derrida: *Physica D*, Elsevier, New York, NY, 1997, pp. 467-77.
35. P.G. Shewmon: *Diffusion in Solids*, McGraw-Hill Series in Materials Science and Engineering, McGraw-Hill, New York, NY, 1963.
36. S. Takeuchi and A.S. Argon: *J. Mater. Sci.*, 1976, vol. 11, pp. 1542-66.
37. O.D. Sherby: *Acta Metall.*, 1962, vol. 10, pp. 135-41.
38. F. Garofalo: *Fundamentals of Creep and Creep-Rupture in Metals*, Macmillan Series in Materials Science, Macmillan, 1965.
39. H. Brehm and G.S. Daehn: *A Model for Slip Creep Based on Coarsening Kinetics*, to be published.
40. O.D. Sherby, R.H. Klundt, and A.K. Miller: *Metall. Mater. Trans. A*, 1977, vol. 8A, p. 843.